

Potential utility of the real-time TMPA-RT precipitation estimates in Streamflow prediction

^{1,2}Fengge Su, ¹Huilin Gao, ³George J. Huffman, and ¹Dennis P. Lettenmaier

¹Department of Civil and Environmental Engineering, University of Washington, Seattle, WA 98195, USA

²Key Laboratory of Tibetan Environment Changes and Land Surface Processes, Institute of Tibetan Plateau Research, Chinese Academy of Sciences, Beijing 100085, China

³Science Systems and Applications, Inc. and NASA/GSFC Laboratory for Atmospheres, Code 613.1, Greenbelt, MD 20771, USA

Corresponding author: Fengge Su (fgsu@itpcas.ac.cn)

Submitted *Journal of Hydrometeorology*

July 30, 2010

ABSTRACT

We investigate the potential utility of the real-time Tropical Rainfall Measuring Mission (TRMM) Multi-satellite Precipitation Analysis (TMPA-RT) data for streamflow prediction, both through direct comparisons of TMPA-RT estimates with a gridded gauge product, and through evaluation of streamflow simulations over four tributaries of La Plata Basin (LPB) in South America using the two precipitation products. Our assessments indicate that the relative accuracy and the hydrologic performance of TMPA-RT-based streamflow simulations generally improved after February 2005. The improvements in TMPA-RT since 2005 are closely related to upgrades in the TMPA-RT algorithm in early February, 2005 which include use of additional microwave sensors (AMSR-E and AMSU-B) and implementation of different calibration schemes. Our work suggests considerable potential for hydrologic prediction using purely satellite-derived precipitation estimates (no adjustments by in situ gauges) in parts of the globe where in situ observations are sparse.

1. Introduction

The emergence of an increasing number of high-resolution (e.g. 0.25-degree latitude-longitude spatially and 3-hourly or higher time frequency) near real-time and quasi-global satellite-based combined precipitation products (e.g., Huffman et al. 2007; Kubota et al. 2007; Turk and Miller 2005; Hong et al. 2004; Joyce et al. 2004; Kidd et al. 2003; Scofield and Kuligowski 2003; Sorooshian et al. 2000) offers the potential to address flood prediction problems in ungauged basins globally (Hong et al. 2007a; Hossain et al. 2007; Hossain and Lettenmaier 2006). Current TRMM-era and future Global Precipitation Measurement (GPM) mission combined precipitation products generally merge geostationary infrared data and polar-orbiting microwave data to take advantage of the frequent sampling of the infrared and the superior quality of the microwave. With respect to hydrometeorological prediction, GPM is intended to improve hydrometeorological models and their application to flood forecasting and seasonal-regional flood-drought outlooks through better temporal sampling and spatial coverage of high-resolution precipitation measurements (Smith et al. 2007). However, given the known errors and uncertainties associated with satellite-based precipitation estimates (Hong et al. 2006; Hossain and Anagnostou 2004; Nijssen and Lettenmaier 2004; Steiner et al. 2003; McCollum et al. 2002), the feasibility of using satellite precipitation as input to hydrology models for flood forecasting and other hydrological prediction purposes remains an open issue. The NASA real-time flood monitoring system based on TRMM-based precipitation and a simple hydrology model (<http://trmm.gsfc.nasa.gov/>; Hong et al. 2007a) suggests the potential for the use of remote sensing data sources for flood hazard prediction globally; however the quantitative rainfall-runoff prediction accuracy of this system has yet to be verified. Before the hydrologic

goal of GPM can be realized and a global flood monitoring capability can be implemented for operational purposes globally, hydrologically-based assessments of satellite precipitation products that are available in real-time (from a practical standpoint, meaning that they do not rely on adjustments based on concurrent in situ data) are needed.

Su et al. (2008) evaluated nine years (1998-2006) of the TRMM Multi-satellite Precipitation Analysis (TMPA) research product (3B42 Version 6, hereafter referred to TMPA-V6; Huffman et al. 2007) using gridded gauge data and the Variable Infiltration Capacity (VIC) semi-distributed hydrology model over La Plata basin (LPB), the sixth largest river basin in the world. The TMPA-V6-driven VIC model simulations were able to capture high flow events at the daily time scale for large tributaries within the LPB, and to represent seasonal and interannual streamflow variability. The authors argued, however, that the encouraging aspects of the hydrologic performance of TMPA research product were substantially attributable to the monthly gauge correction applied to TMPA-V6, a correction that requires a reasonably dense gauge network, and cannot be performed in real-time. In contrast, satellite-based estimates are expected to be most useful for hydrologic prediction in river basins where dense gauge networks do not exist.

In this study we extend the work reported in Su et al. (2008) by evaluating the TMPA real-time product 3B42RT (hereafter referred to as TMPA-RT) that is derived from satellite data alone. We compare the TMPA-RT data with a gridded gauge product, and compare streamflow simulations using the VIC model forced both with the satellite data and a gridded gauge product. The purpose of this study is to investigate the evolution of the performance of current real-time satellite precipitation products and to understand the current level of accuracy that can be achieved for hydrologic prediction using global satellite precipitation datasets.

2. Data and Methodology

Microwave imagers and sounders have a direct physical connection to the hydrometeor profiles above the surface, but suffer from poor temporal sampling. In contrast, geo- infrared (IR) data provide excellent time-space coverage, however their relationship to precipitation is indirect. The TMPA estimates are based on passive microwave (PMW) data provided by various low-orbiting satellites, merged with microwave-calibrated IR-based estimates from geostationary meteorological satellites to fill PMW coverage gaps (Huffman et al. 2007; 2010). The sources of microwave data in the TMPA include the TRMM Microwave Imager (TMI), Special Sensor Microwave Imager (SSM/I) on Defense Meteorological Satellite Program (DMSP) satellites, Advanced Microwave Scanning Radiometer-Earth Observing System (AMSR-E) on Aqua, the Advanced Microwave Sounding Unit-B (AMSU-B) on the National Oceanic and Atmospheric Administration (NOAA)-15, 16, and 17 satellites, and the Microwave Humidity Sounder-based precipitation estimates from NOAA-18 (which replaced the AMSU-B on board previous NOAA satellites). For TMPA, the PMW data are first calibrated using the TRMM Combined Instrument (TCI; which combines data from both TMI and the PR data), and then used to calibrate the IR input.

It is important to note that only SSM/I and TMI (2A12RT) estimates were incorporated in the combined microwave (or high quality, HQ) product prior to 3 February 2005. At that point, precipitation estimates from AMSR-E and the three AMSU-B sensors were introduced. NOAA-18 data were added to TMPA-RT starting on 27 November 2007 (ftp://trmmopen.gsfc.nasa.gov/pub/merged/3B4XRT_README.pdf). These changes nearly doubled the typical combined microwave coverage in the latitude band 50° N-50° S from ~45%

to nearly 80%. Two other important upgrades were also made to TMPA-RT on 3 February 2005:

- 1) Inter-satellite calibration of the HQ product (to TMI) became climatological, reducing the real-time computational load and preparing for the eventual termination of TRMM; and
- 2) the microwave-calibrated IR coefficients began to be recomputed every 3 hours to better control unrealistically high estimates when unusually cold IR Tbs are encountered in a region.

Knowledge of these upgrades is important to understanding the evolution of the TMPA-RT performance and its potential for hydrologic prediction. Although the developers consider the datasets produced before 3 February 2005 to be obsolete, it is instructive to examine the change in skill that resulted from the changes noted above.

The TMPA-RT product was released from February 2002 on. Our period of analysis is January 1, 2003 through December 31, 2008. All the TMPA-RT data are at a 0.25-degree grid and a 3-hour time-step. The gridded gauge precipitation for 2003-08 at 0.25 degree for the LPB was provided by Drs. Brant Liebmann and Dave Allured as a regridding of their South American gridded daily precipitation product on 1-degree and 2.5-degree grids (methods described in Liebmann and Allured 2005). The VIC model setup (e.g., soil and vegetation parameter files) was taken from Su et al. (2008).

Precipitation gauge distributions within our study area for 2003-2008 are shown in Fig. 1. We performed our evaluations on four highlighted subbasins of La Plata basin where there was relatively dense station coverage (except for 2008). Triangles on Fig.1 are streamflow stations; the numbers are station IDs (6682, 6301, 6598, and 3802) and also represent the basins upstream of the stations (see Table 1 for drainage area). Daily precipitation estimates from the TMPA-RT and gridded gauge observations were used to force the VIC hydrology model over the four subbasins for 2003-2008. The daily basin-wide precipitation estimates from TMPA-RT were

compared with those from gauge observations, and the TMPA-RT-driven and gridded gauge-driven modeled streamflow were compared with each other and with streamflow observations where available. Due to the sparse gauge network density in 2008 (Fig. 1), analysis of precipitation and simulated streamflow mostly focused on the period 2003-2007.

3. Evaluation of TMPA-RT Precipitation Estimates

Our evaluation aims to understand the evolution of the performance of the TMPA-RT estimates and the skill of the real-time satellite estimates in detecting the amount and timing of rainy events at basin scales.

a. Evolution of the performance of the TMPA-RT estimates

The quantitative accuracy of satellite precipitation estimation was assessed using the correlation coefficient (R^2), relative mean bias (defined as $\text{Bias} = [(\overline{P}_s - \overline{P}_g) / \overline{P}_g] \times 100\%$, where \overline{P}_s and \overline{P}_g are mean satellite-based and gauge-based precipitation estimates), and normalized root-mean-square error ($\text{Nrmse} = \sqrt{\sum_{i=1}^{i=n} (P_{si} - P_{gi})^2 / n} / \overline{P}_g$, where P_{si} and P_{gi} denote satellite and gauge daily basin-wide precipitation estimates, and n is the number of precipitation pairs in the analysis). Fig. 2 shows scatterplots of daily basin-averaged precipitation from TMPA-RT relative to gridded gauge estimates over the four selected sub-basins in LPB for each year from 2003 to 2007. Statistical results are shown in Table 1.

Basins 3802 and 6598 are located in the central portion of the LPB (Fig. 1), where the precipitation regime is mostly affected by mesoscale convective systems and transient activity leading to irregular characteristics with precipitation maxima appearing in all seasons of the year (Berbery and Barros 2002). TMPA-RT tended to overestimate the gauge values over these two

central basins especially for 2003 and 2004 (Bias of 28-56%) in spite of relative high R^2 (0.66~0.79). The performance of TMPA-RT over basins 3802 and 6598 substantially improved for 2005-2007 with decreased Bias (10-30%) and Nrmse (60~150%) (Fig. 2, Table 1).

Basin 6301 (Fig. 1) has a well-defined precipitation regime which is related to the South American monsoon system, with the rainy season occurring in austral summer (December–February) and a dry season in winter (June–August). Biases of basin 6301 in 2005-2007 (-3~3%) did not show improvements compared with 2004 (-2%), however R^2 increased from 0.67~0.75 in 2003-2004 to 0.76~0.87 in 2005-2007, and the mean Nrmse of 2005-2007 decreased about 20% compared with that of 2003-2004.

Basin 6682 (Fig. 1) is located in the upstream portion of the Paraguay River (one of the three major tributaries of La Plata), and includes the world's largest wetland (Pantanal). The TMPA-RT performance over this basin showed consistent improvements for 2005-2007 relative to 2003-2004 in terms of R^2 , Bias, and Nrmse (Table 1), although basin 6682 has the worst agreement between TMPA-RT and the gauge produce (mean R^2 of 0.52 for 2003-2004, and 0.68 for 2005-2007) among the four selected basins. The poor correspondence between the satellite and gauge estimates in basin 6682 might be related to the existence of large wetland areas within the basin. Tian et al. (2007) found systematic anomalies in TMPA-V6 and CMORPH precipitation estimates over inland water bodies in the southeastern U.S. They speculated that the anomalies are caused by deficiencies in the passive microwave-based rainfall retrieval representation of emissivity over water versus land.

Scatterplots (Fig.3) of monthly basin-averaged accumulations of gridded gauge and TMPA-RT estimates over the selected basins suggest apparent improvements in 2005-2008 in terms of

both bias and R^2 . The mean biases decreased 5~30% in 2005-2008 compared with 2003-2004, and R^2 increased from 0.74~0.88 in 2003-2004 to 0.84~0.94 in 2005-2008.

The above analysis suggests that the performance of TMPA-RT data substantially improved after 2005 over the four selected subbasins in LPB. As mentioned in Section 2, several important upgrades occurred to TMPA-RT in February 2005, including better spatial coverage from microwave sensors (AMSR-E and AMSU-B) and implementation of different calibration schemes.

b. Evaluation of TMPA-RT in detecting rainy events

The frequency bias index (FBI), probability of detection (POD), false alarm ratio (FAR), and equitable threat score (ETS) based on a 2×2 contingency table (a: satellite yes, observation yes; b: satellite yes, observation no; c: satellite no, observation yes; and d: satellite no, observation no; Wilks 1995) were used to quantify the skill of the daily TMPA-RT accumulations in detecting rainy events. All these indicators were calculated based on basin average precipitation. The FBI $[(a + b)/(a + c)]$ indicates whether there is a tendency to underestimate (FBI < 1) or overestimate (FBI > 1) the occurrence of rainy events. The FAR $[b/(a + b)]$ measures the fraction of rain detections that were actually false alarms. The POD $[a/(a + c)]$ gives the fraction of rain occurrences that were correctly detected. The ETS $[(a - H_e)/(a + b + c - H_e)]$ gives the overall fraction of correctly diagnosed events by the TMPA-RT algorithm, where $H_e = (a + c)(a + b)/N$ and N is the total number of estimates. Perfect values for these scores are FBI=1, FAR = 0, POD = 1, and ETS = 1. To evaluate the skill of the daily TMPA-RT estimates for light and heavy rainfall events, the FAR, FBI, POD, and ETS were calculated for

precipitation thresholds of 0.1, 0.5, 1, 2, 5, 10, and 20 mm day⁻¹. Given the apparent bias found in TMPA-RT in 2003-2004, the analysis in this Section only uses the data for 2005-2007.

Fig. 4 shows the verification results for FBI, FAR, POD, and ETS for the four sub-basins highlighted in Fig. 1 for the period 2005- 2007. TMPA-RT tended to overestimate the frequency of rain events for the thresholds greater than 10 mm over the central basin 3802 and northern basin 6682, and overestimated the rain events over all the basins for rain rate more than 20mm day⁻¹ (Fig. 4a). FAR started becoming large (0.2-0.8) for precipitation threshold greater than 10mm for all the basins with the largest FAR appearing over basin 6682 (Fig. 4b). For the two northern basins (6301 and 6682), rain occurrence was best detected for precipitation thresholds up to 2mm (POD >0.85), and the skill rapidly dropped with increasing precipitation thresholds (Fig. 4c). The two central basins (6598 and 3802) showed increasing POD scores (0.7–0.9) for the thresholds up to 5mm, than the POD scores started dropping for the higher thresholds.

Fig. 4d showed the overall skill (ETS) of TMPA-RT over the four subbasins. In general, basin 6682 had the lowest ETS values (0.2-0.55) among the selected basins for all the precipitation thresholds, and basin 6301 had the highest ETS (0.6-0.8) for thresholds up to 2 mm. The two central basins (3802 and 6598) showed consistent trends of ETS with those of POD, with the best ETS scores (around 0.7) for the threshold 5mm. All basins showed deteriorating scores (FBI, FAR, POD, and ETS) for thresholds more than 5mm, suggesting that TMPA-RT tended to have higher uncertainties for medium to high precipitation rates over these basins. The strong performance of TMPA-RT for basin 6301 is partly due to the relatively larger area leading to smoothing of precipitation variation and errors (Nijssen and Lettenmaier 2004).

In the work of Su et al. (2008), TMPA-V6 showed good performance in tracking the monthly variations of gauged precipitation over the subbasins in the LPB. The authors argued

that this was mostly because of the monthly gauge adjustments included in TMPA-V6. To investigate the performance of the purely satellite-derived TMPA-RT in detecting interannual variations and seasonal cycle of basin-averaged precipitation, Fig.5 shows monthly time series of precipitation from gauge and TMPA-RT estimates for the periods 2003-2008 over the four subbasins (for comparison purposes, the results from TMPA-V6 are also included). For the years 2005-2007, TMPA-RT tracks the monthly variations of gauged estimates well over all the basins, especially basin 6301 (Fig. 5c) with nearly zero bias and R^2 of 0.94 (Fig. 3). The TMPA-RT in general tended to overestimate gauge observations over the two central basins (3802, 6598) for most of the months with high rainfall, and tended to overestimate precipitation for the first half of the water year (Jul-Dec) over the northern basin 6682. Given the fact that there are no gauge adjustments included in the real-time version of TMPA, the performance of TMPA-RT with respect to representation of monthly precipitation variations is encouraging.

3.1 Evaluation of Streamflow Predictions

To investigate the utility of the real-time satellite precipitation estimates for streamflow prediction, both gridded TMPA-RT and gauge estimates were used to force the VIC model. The VIC model was calibrated and tested for the major subbasins of LPB for the period 1979-1999 by Su and Lettenmaier (2009). We used the calibrated VIC parameters from the prior study and forced the model with daily precipitation estimates from both TMPA-RT and gridded gauge observations for 2003-2008 over the four selected basins. Observed daily streamflow was only available for basin 3802 (Uruguay at Paso de los Libres) for 2003-2007. The gauge-driven VIC-simulated streamflow was used as a reference for the other basins (6598, 6301, 6682), which allowed us to investigate how differences between TMPA-RT and gauge precipitation estimates

affect the resulting simulated streamflow. The Nash-Sutcliffe efficiency

$$(Ef = 1 - \frac{\sum (Q_{oi} - Q_{ci})^2}{\sum (Q_{oi} - \overline{Q_o})^2}, \text{ where } Q_{oi} \text{ and } Q_{ci} \text{ are observed and simulated}$$

streamflow on day i , and $\overline{Q_o}$ is daily mean of observed streamflow) and relative error

$$(Er = \frac{\overline{Q_c} - \overline{Q_o}}{\overline{Q_o}}, \text{ where } \overline{Q_c} \text{ is daily mean of simulated streamflow) were used to evaluate the}$$

hydrological performance of the satellite data. Table 2 summarizes the Nash-Sutcliffe efficiency

(Ef) and relative errors (Er) relative to observed or gauge-driven modeled streamflow for 2005-

2007. Figs. 6-9 show daily VIC simulated streamflow forced by TMPA-RT and gridded gauge

precipitation estimates for basins 3802, 6598, 6301, and 6682 for 2003-2008. To show the

difference in VIC performance when the research and real-time products were used to force the

hydrology model, the TPMA-V6-driven VIC model simulations were also included in Figs. 6-9.

Fig. 6 shows predicted and observed daily streamflow for station 3802 (the Uruguay River at Paso de los Libres, drainage area 189 300 km²). The gauge-driven simulations at station 3802 tracked the high variation of the observed daily hydrograph well for 2003-2006, which was consistent with the good performance of the VIC model over the Uruguay basin in earlier years (Su et al. 2008; Su and Lettenmaier 2009). The gauge-driven simulated streamflow overestimated the observations by 28% in 2007 alone, likely due to the uncertainties in the gridded gauge precipitation inputs to the VIC hydrology model for that year.

TMPA-RT-driven simulations overestimated the observed streamflow by more than 100% in 2003 and 2004 for basin 3802 (Fig. 6), while the mean relative error in TMPA-RT-driven runs substantially decreased in 2005-2007 (Er of 67% and 42% relative to the observed streamflow and the gauge-driven runs respectively, Table 2). 2006 was a dry year for basin 3802 and there was large positive bias in the TMPA-RT precipitation estimates (33%, Fig. 1) over this basin,

which resulted in larger errors in the simulated runoff (82%) in 2006. In spite of the overestimation, the TMPA-RT-driven model simulations tracked the high variation of the daily hydrographs for the basin 3802 in the post-2004 years. Table 2 and Figure 6 also suggest the reduction of errors in the TMPA-V6-driven simulations (Er of 22-43%) due to the inclusion of the gauge adjustment, which exhibited closer agreement with both the observed and gauge-driven simulations (model efficiency of 0.73-0.75) than the TMPA-RT data.

Basin 6598 (Iguazu at Estreito), with a drainage area of 63 200 km², has an irregular streamflow regime with floods of short duration occurring at any time of the year (Fig.7). The hydrologic performance of TMPA-RT for basin 6598 was similar to that of basin 3802. The TMPA-RT-driven simulated streamflow overestimated the gauge-driven runs by 66% during 2003-2004, while the mean bias substantially decreased in 2005-2007 (mean model efficiency of 0.74 and Er of 16%, Table 2). The TMPA-RT-driven simulations agree surprisingly well with the gauge-driven runs in the occurrence of high variable daily flooding events for the 2005-2007. The TMPA-RT-driven runs showed comparable hydrologic performance with the TMPA-V6 for the same period in term of model efficiency and Er (Table 2), suggesting the promising potential of satellite-based precipitation in hydrologic prediction.

Fig. 8 shows daily simulated hydrographs for station 6301 (Paraná at Jupia; drainage area 478 000 km²), where there is a well-defined streamflow regime. Inconsistencies between modeled hydrographs driven by the TMPA-RT and gauges in both timing and magnitude of daily flows for the period Jan 2003- Jan 2005 can be seen in Fig. 8. The agreement between TMPA-RT and gridded gauge-driven simulations substantially improved after Jan 2005 with model efficiency of 0.91 and relative error of -5% for Feb 2005-Dec 2007. The hydrologic performance

of TMPA-RT was even better than the TMPA-V6 for the period Feb 2005-Dec 2007 in terms of the model efficiency and relative error (Table 2).

Daily simulated hydrographs for station 6682 (Paraguay River at Ladario; drainage area 459 990 km²) is shown in Fig. 9. Due to the wet soil conditions in this basin (which has large wetland areas), the large positive bias in the TMPA-RT precipitation input (Table 1) was transformed into a larger positive bias in the simulated streamflow (Table 2). The TMPA-RT-driven simulations were consistently higher than the observation-driven simulations for almost the entire period, however the TMPA-RT-driven runs did show better agreement with gridded gauge-driven simulated streamflow in 2006 and 2007, with the best agreement occurring in 2007 (model efficiency of 0.65 and relative error of 19% for 2007).

4. Conclusions and Recommendations

The objective of this study was to evaluate the potential utility of purely satellite-derived precipitation estimates for hydrologic prediction, as they may provide the only source of precipitation for areas where ground-based networks are unavailable. We compared the basin-averaged precipitation from the TMPA-RT and gauge estimates, and the VIC hydrologic model simulated streamflow driven by both gridded TMPA-RT and gauge precipitation inputs over four selected subbasins in the LPB. Our assessments indicate that the relative accuracy and the hydrologic performance of TMPA-RT generally improved after February 2005. Our general conclusions are as follows:

- 1) The TMPA-RT showed substantially decreased Bias and Nrmse over the two central convective-system-dominated basins (3802, 6598) and had better correspondence with

the gauge estimates over the northern basin 6301 for 2005-2007 compared with 2003-2004.

- 2) In spite of the improvement of TMPA-RT in 2005-2007, TMPA-RT tended to overestimate the frequency of rainy events for rain rates greater than 10-20 mm/d and the false alarm ratio was quite high for those precipitation thresholds, especially over the northern basin 6682, which has large area of wetlands.
- 3) Monthly precipitation variations of gauge estimates were well tracked by the TMPA-RT estimates over all the selected subbasins (especially basin 6301) for the period 2005-2007.
- 4) The TMPA-RT-driven model simulations tracked the high variations of the daily hydrographs very well for the two central basins (basins 3802 and 6598) in the post-2004 years, and showed comparable hydrologic performance with TMPA-V6 for the same period in term of model efficiency and relative error. For the northern basin 6301, TMPA-RT outperformed the TMPA-V6 for the period Feb 2005-Dec 2007 with gauge-driven runs as the reference. Large uncertainties occurred in basin 6682 (which has a large wetland area), however the TMPA-RT-driven runs showed improved agreement with gridded gauge-driven simulated streamflow in 2006 and 2007.

Our analysis suggests considerable potential for hydrologic prediction using purely satellite-derived (no in situ gauge adjustment) precipitation estimates in parts of the globe where in situ observations are sparse. Clearly, satellite-based estimates that rely on gauge corrections, such as TMPA-V6, can only be as good as the gauge estimates that form the basis for the corrections. Furthermore, monthly corrections preclude the use of the products for real-time applications. As mentioned in Section 2, several important upgrades occurred to TMPA-RT in February 2005, including better spatial coverage from microwave sensors (AMSR-E and AMSU-B) and

implementation of different calibration schemes. The improved performance of TMPA-RT from 2005 onward is presumed to be related to these upgrades. The planned GPM mission, which consists of a constellation of low earth orbiting satellites carrying various passive and active microwave measuring instruments, aspires to facilitate a quantum leap relative to current state-of-the-art satellite precipitation products through improving measurement accuracy, sampling frequency, and global coverage.

A natural extension of this work is to perform evaluations over different hydroclimatic regions (e.g., semiarid, high altitude area) with varying basin sizes and rain gauge network densities to further test the possible benefits of using satellite-based precipitation estimates for flow prediction. In this respect, the work we report here could serve as a template for hydrologically-based evaluation of satellite precipitation products elsewhere.

Acknowledgments. The authors thank Brant Liebmann and Dave Allured for providing the 0.25° gridded precipitation data for the La Plata basin. We also thank Yang Hong and Jiahu Wang for technical assistance, and William L. Crosson for his helpful comments. This work was supported by the National Aeronautics and Space Administration under Grant NNX08AO34G to the University of Washington.

REFERENCES

- Berberly, E. H., and V. R. Barros, 2002: The hydrologic cycle of the La Plata basin in South America. *J. Hydrometeor.*, **3**, 630–645.
- Hong, Y., K. L. Hsu, X. Gao, and S. Sorooshian, 2004: Precipitation estimation from remotely sensed imagery using artificial neural network - cloud classification system (PERSIANN-CCS), *J. Appl. Meteor.* **43**, 1834–1853.
- Hong, Y., K.-L. Hsu, H. Moradkhani, and S. Sorooshian, 2006: Uncertainty quantification of satellite precipitation estimation and Monte Carlo assessment of the error propagation into hydrologic response. *Water Resources Res.*, **42**, W08421, doi:10.1029/2005WR004398.
- Hong, Y., R. F. Adler, F. Hossain, S. Curtis, and G. J. Huffman, 2007a: A first approach to global runoff simulation using satellite rainfall estimation, *Water Resources Res.*, **43**, W08502, doi: 10.1029/2006WR005739.
- Hong, Y, R. F. Adler, A. Negri, and G. J. Huffman, 2007b: Flood and landslide applications of near real-time satellite rainfall estimation, *Natural Hazards* (Special Issue), **43**, doi: 10.1007/s11069-006-9106-x, 285-294.
- Hossain, F., and E. N. Anagnostou, 2004: Assessment of current passive-microwave- and infrared-based satellite rainfall remote sensing for flood prediction, *J. Geophys. Res.*, **109**, D07102, doi:10.1029/2003JD003986.
- Hossain, F., and D.P. Lettenmaier, 2006: Flood prediction in the future: Recognizing hydrologic issues in anticipation of the Global Precipitation Measurement mission. *Water Resources Res.*, **42**, W11301, doi:10.1029/2006WR005202.
- Hossain, F., N. Katiya, A. Wolf, and Y. Hong, 2007: The Emerging role of Satellite Rainfall Data in Improving the Hydro-political Situation of Flood Monitoring in the Under-developed

Regions of the World, *Natural Hazards* (Special Issue), **43**, doi 10.1007/s11069-006-9094-x, 199-210.

Huffman, G. J., R. F. Adler, D. T. Bolvin, G. Gu, E. J. Nelkin, K. P. Bowman, Y. Hong, E. F. Stocker, and D. B. Wolff, 2007: The TRMM Multi-satellite Precipitation Analysis (TMPA): Quasi-Global, Multi-Year, Combined-Sensor Precipitation Estimates at Fine Scales. *J. Hydrometeor.*, **8**, 38-55.

Huffman, G. J., R. F. Adler, D.T. Bolvin, and E.J. Nelkin, 2010: The TRMM Multi-Satellite Precipitation Analysis (TMPA), Gebremichael, M., F. Hossain (eds.), *Satellite Rainfall Applications for Surface Hydrology*, DOI 10.1007/978-90-481-2915-7_1, Springer Science+Business Media B.V.

Joyce, R. J., J. E. Janowiak, P. A. Arkin and P. Xie, 2004: CMORPH: A method that produces global precipitation estimates from passive microwave and infrared data at high spatial and temporal resolution. *J. Hydrometeor.*, **5**, 487–503.

Kidd, C. K., D. R. Kniveton, M. C. Todd, and T. J. Bellerby, 2003: Satellite rainfall estimation using combined passive microwave and infrared algorithms. *J. Hydrometeor.*, **4**, 1088–1104.

Kubota T, Shige S, Hashizume H, Aonashi K, Takahashi N, Seto S, Hirose M, Takayabu YN, Nakagawa K, Iwanami K, Ushio T, Kachi M, Okamoto K (2007) Global precipitation map v using satellite-borne microwave radiometers by the GSMaP Project: Production and validation. *IEEE Trans. Geosci. Remote Sens.* **45**:2259–2275

Liebmann, B., and D. Allured, 2005: Daily precipitation grids for South America, *Bull. Amer. Meteor. Soc.*, **86**, 1567-1570.

- McCollum, J. R., W. F. Krajewski, R. R. Ferraro, and M. B. Ba, 2002: Evaluation of biases of satellite estimation algorithms over the continental United States. *J. Appl. Meteor.*, **41**, 1065–1080.
- Nijssen, B., and D. P. Lettenmaier, 2004: Effect of precipitation sampling error on simulated hydrological fluxes and states: Anticipating the Global Precipitation Measurement satellites. *J. Geophys. Res.*, **109**, D02103, doi: 10.1029/2003JD003497.
- Sorooshian, S., K. Hsu, X. Gao, H. Gupta, B. Imam, and D. Braithwaite, 2000: Evaluation of PERSIANN System Satellite-Based Estimates of Tropical Rainfall. *Bull. Amer. Meteor. Soc.*, **81**, 2035-2046.
- Smith, E., et al., 2007: The International Global Precipitation Measurement (GPM) program and mission: An overview, in *Measuring Precipitation From Space: EURAINSAT and the Future*, edited by V. Levizzani and F. J. Turk, Springer, New York, 611-653.
- Scofield, R. A., and R. J. Kuligowski, 2003: Status and outlook of operational precipitation algorithms for extreme precipitation events. *Wea. Forecasting*, **18**, 1037 - 1051.
- Steiner, M., T. L. Bell, Y. Zhang, and E. F. Wood, 2003: Comparison of two methods for estimating the sampling-related uncertainty of satellite rainfall averages based on a large radar data set. *J. Climate*, **16**, 3759–3778.
- Su, F., H. Yang, and D. P. Lettenmaier, 2008: Evaluation of TRMM Multi-satellite Precipitation Analysis (TMPA) and its utility in hydrologic prediction in La Plata Basin, *J. Hydrometeorol.*, **9**, 622-640.
- Su, F., and D. P. Lettenmaier, 2009: Estimation of surface water budget of La Plata Basin. *J. Hydrometeorol.* **10**, 981-998.

Turk, F. J., and S.D. Miller, 2005: Toward improving estimates of remotely-sensed precipitation with MODIS/AMSR-E blended data techniques. *IEEE Trans. Geosci. Rem.Sensing*, **43**, 1059-1069.

Figure Captions

FIG. 1. Precipitation gauge distribution for 2003-2008 over the La Plata Basin. The four subbasins with relatively dense station coverage are highlighted with colors. Triangles represent locations of the outlets of the four highlighted basins. Numbers (6682, 6301, 6598, and 3802) are station IDs.

FIG. 2. Scattergrams of daily basin-averaged precipitation (mm day^{-1}) from TMPA- RT vs. gridded gauge estimates for the four sub-basins shown in Fig. 1 for 2003-2007.

FIG. 3. Scattergrams of monthly basin-averaged precipitation (mm month^{-1}) from TMPA- RT vs. gridded gauge estimates for the four sub-basins shown in Fig. 1 for 2003-2004 and 2005-2008.

FIG. 4. (a) FBI, (b) FAR, (c) POD, and (d) ETS, all calculated for seven daily precipitation thresholds (mm day^{-1}) over four subbasins in La Plata for 2005-2007.

FIG. 5. Monthly time series of basin-averaged precipitation (mm month^{-1}) from TMPA-V6, TMPA-RT, and gauge-based estimates over four subbasins in the La Plata for 2003-2008.

FIG. 6. Daily VIC simulated streamflow forced by TMPA-RT, TMPA-V6, and gridded gauge precipitation estimates for 2003-2008 for station 3802 (Uruguay at Paso de los Libres).

FIG.7. Same as Fig.6 but for basin 6598 (Iguazu at Estreito).

FIG 8. Same as Fig.6 but for basin 6301 (Parana at Jupia).

FIG. 9. Same as Fig.6 but for basin 6682 (Paraguay at Ladario).

Table 1. Statistical summary of the comparison between TMPA-RT and gauge-based daily basin-averaged precipitation estimates over four subbasins in the La Plata Basin for 2003-2007

Basin ID		3802	6598	6301	6682
River/Station		Paraguay/Ladari	Iguazu/Estreito	Parana/Jupia	Paraguay/Ladario
Drainage area (km ²)		189, 300	62, 236	478, 000	459, 990
R ²	2003	0.79	0.76	0.75	0.60
	2004	0.78	0.66	0.67	0.42
	2005	0.77	0.80	0.76	0.68
	2006	0.85	0.79	0.83	0.70
	2007	0.77	0.72	0.87	0.66
	2005-2007	0.79	0.76	0.81	0.68
Nrmse (%)	2003	230	184	87	166
	2004	265	200	84	186
	2005	117	118	79	110
	2006	124	124	55	86
	2007	106	117	54	95
	2005-2007	115	120	64	96
Bias (%)	2003	56	35	18	39
	2004	54	28	-2	27
	2005	21	11	3	22
	2006	33	20	0	16
	2007	20	0	-3	5
	2005-2007	36	9	0	14

Table 2. Nash-Sutcliffe Efficiency (NSE) and Relative Error (Er) of the satellite-driven simulated daily streamflows relative to observed streamflow or gauge-observation-driven simulations for basins 3802, 6598, 6301, and 6682.

	3802				6598		6301		6682	
Precip Input	vs. observed streamflow		vs. gauge-driven simulations		vs. gauge-driven simulations					
	NSE	Error	NSE	Er	NSE	Er	NSE	Er	NSE	Er
TMPA-RT(2005-07)	<0	0.67	0.1877	0.42	0.7380	0.16	0.9116	-0.05	<0	0.75
*TMPA-V6	0.2706/ 0.3326	0.43/ 0.37	0.7349/ 0.7555	0.22/ 0.24	0.7594/ 0.7094	0.09/ 0.15	0.8604/ 0.8404	0.14 0.16	0.8268/ 0.8447	0.10/ 0.10
*Gauged precip	0.6282/ 0.6586	0.18/ 0.11								

*The first number was based on daily data for 2005-2007 and the second was based on data for 2003-2007.

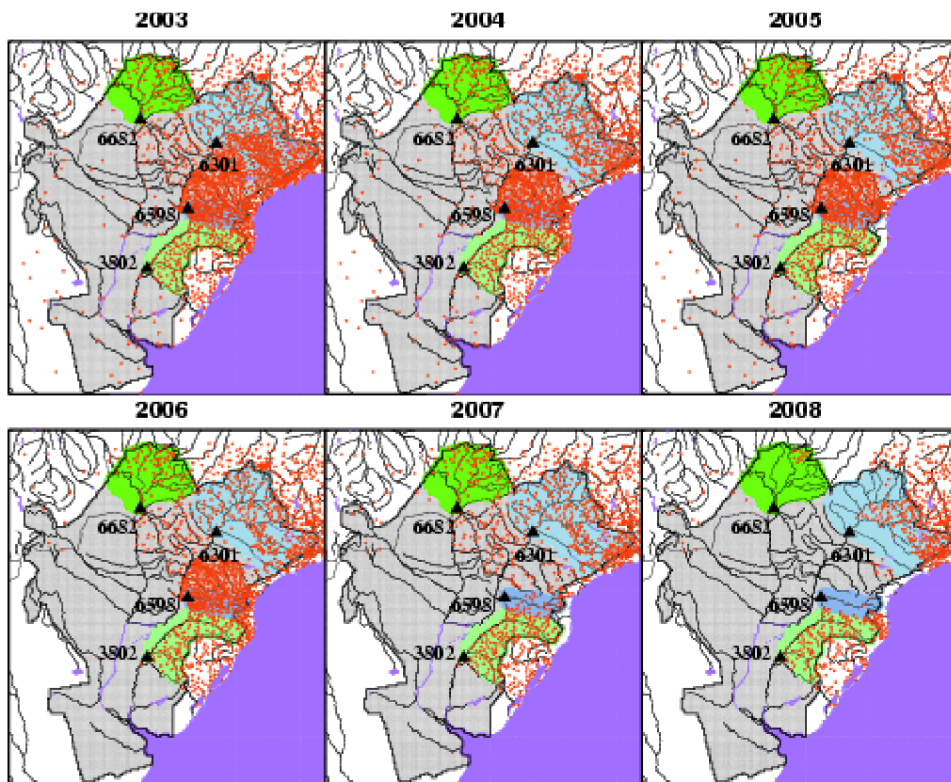


FIG. 1. Precipitation gauge distribution for 2003-2008 over the La Plata Basin. The four subbasins with relatively dense station coverage are highlighted with colors. Triangles represent locations of the outlets of the four highlighted basins. Numbers (6682, 6301, 6598, and 3802) are station IDs.

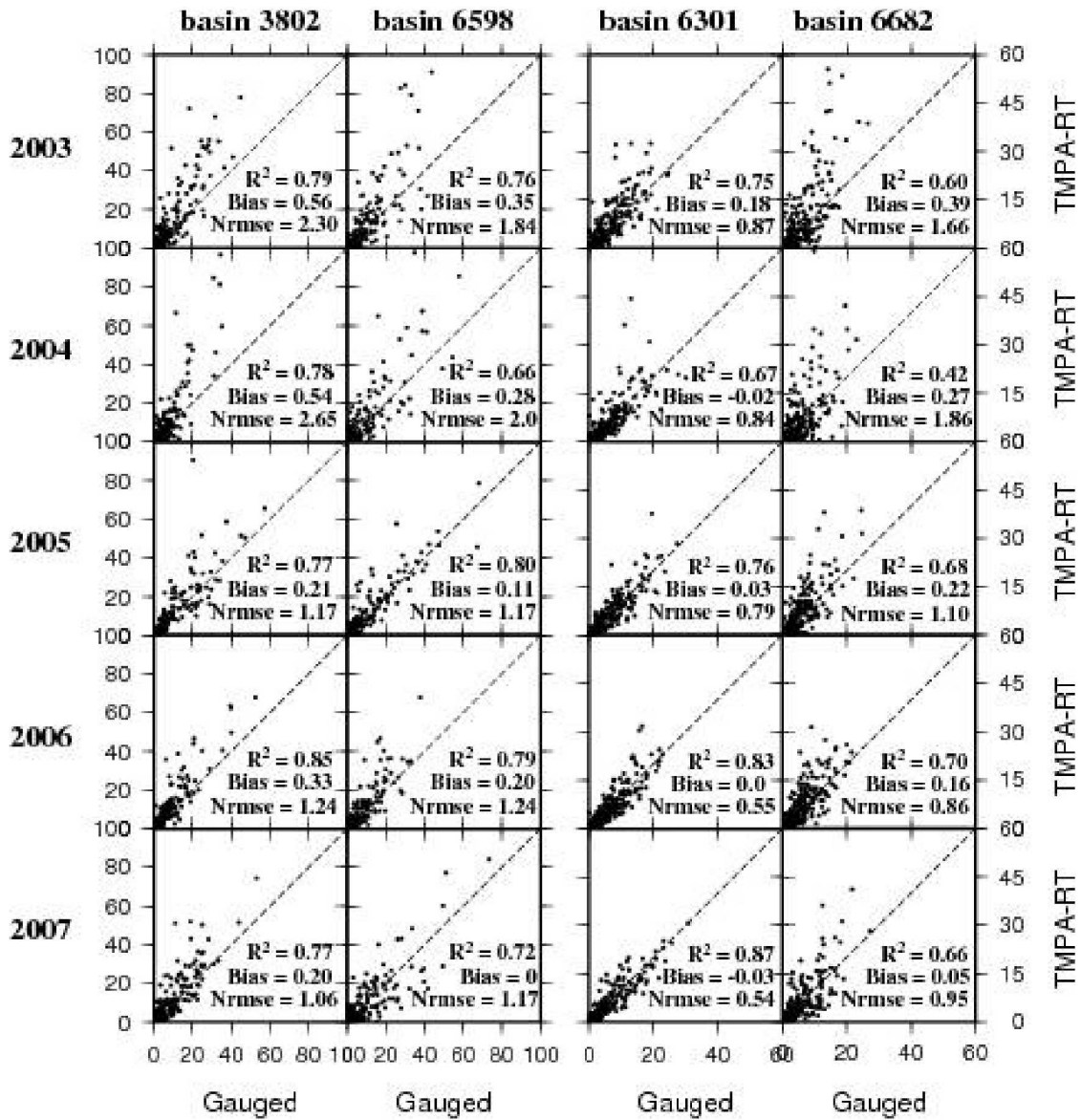


FIG. 2. Scattergrams of daily basin-averaged precipitation (mm day^{-1}) from TMPA-RT vs. gridded gauge estimates for the four sub-basins shown in Fig. 1 for 2003-2007.

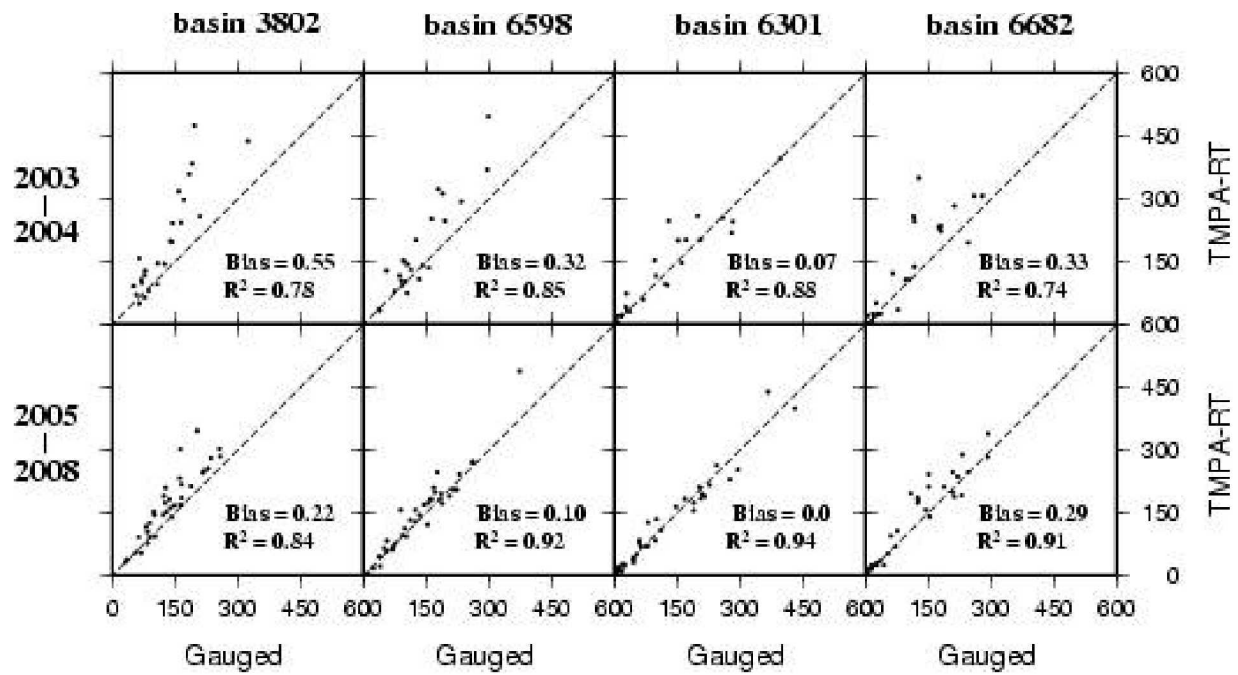


FIG. 3. Scattergrams of monthly basin-averaged precipitation (mm month^{-1}) from TMPA- RT vs. gridded gauge estimates for the four sub-basins shown in Fig. 1 for 2003-2004 and 2005-2008.

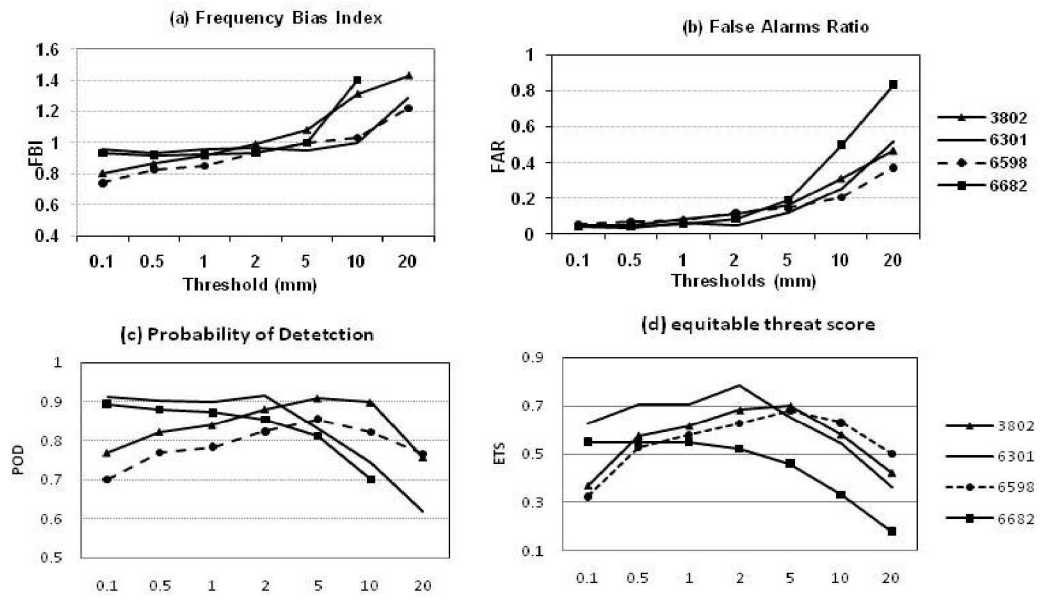


FIG. 4. (a) FBI, (b) FAR, (c) POD, and (d) ETS, all calculated for seven daily precipitation thresholds (mm day^{-1}) over four subbasins in La Plata for 2005-2007.

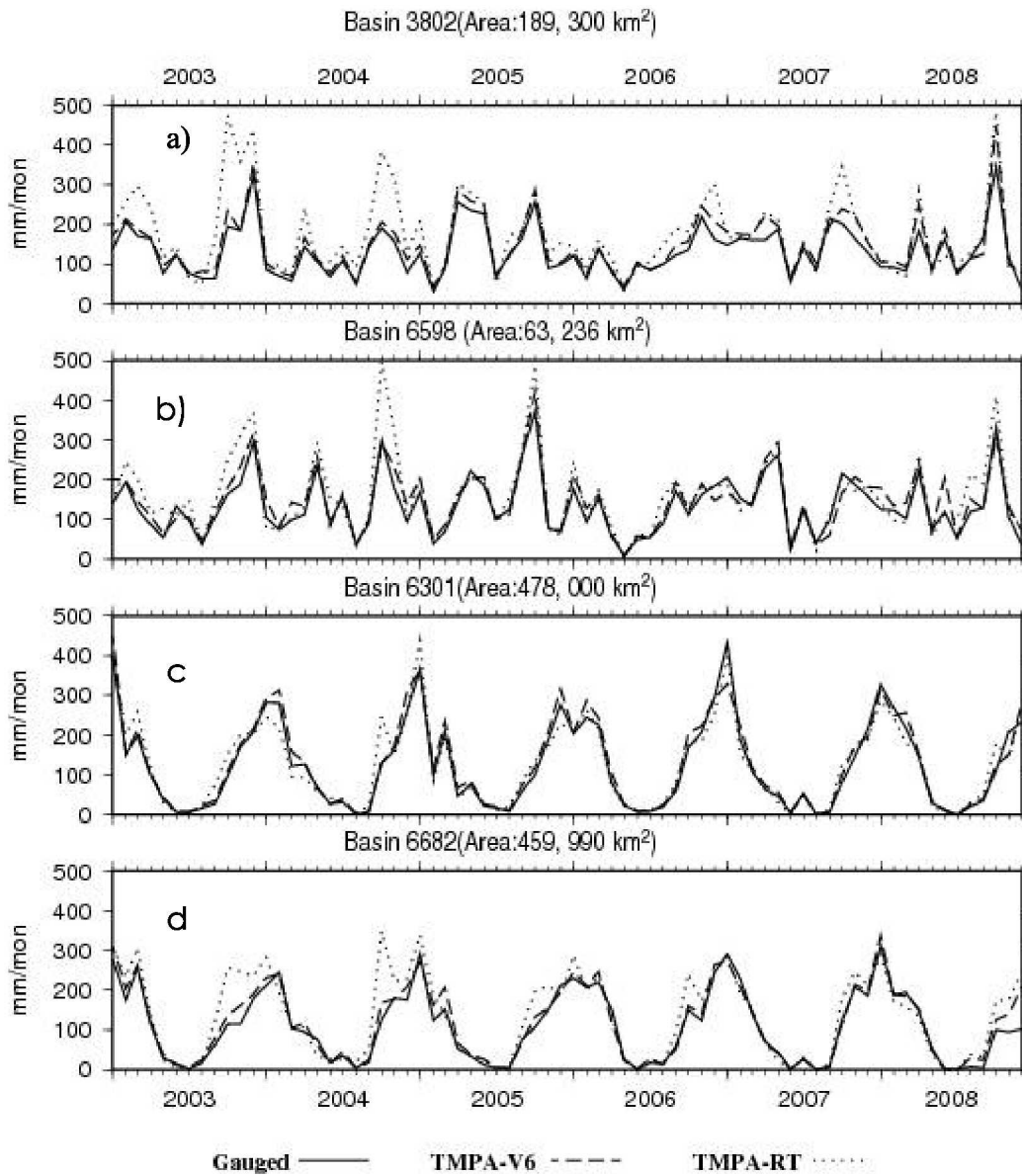


FIG. 5. Monthly time series of basin-averaged precipitation (mm month⁻¹) from TMPA-V6, TMPA-RT, and gauge-based estimates over four subbasins in the La Plata for 2003-2008.

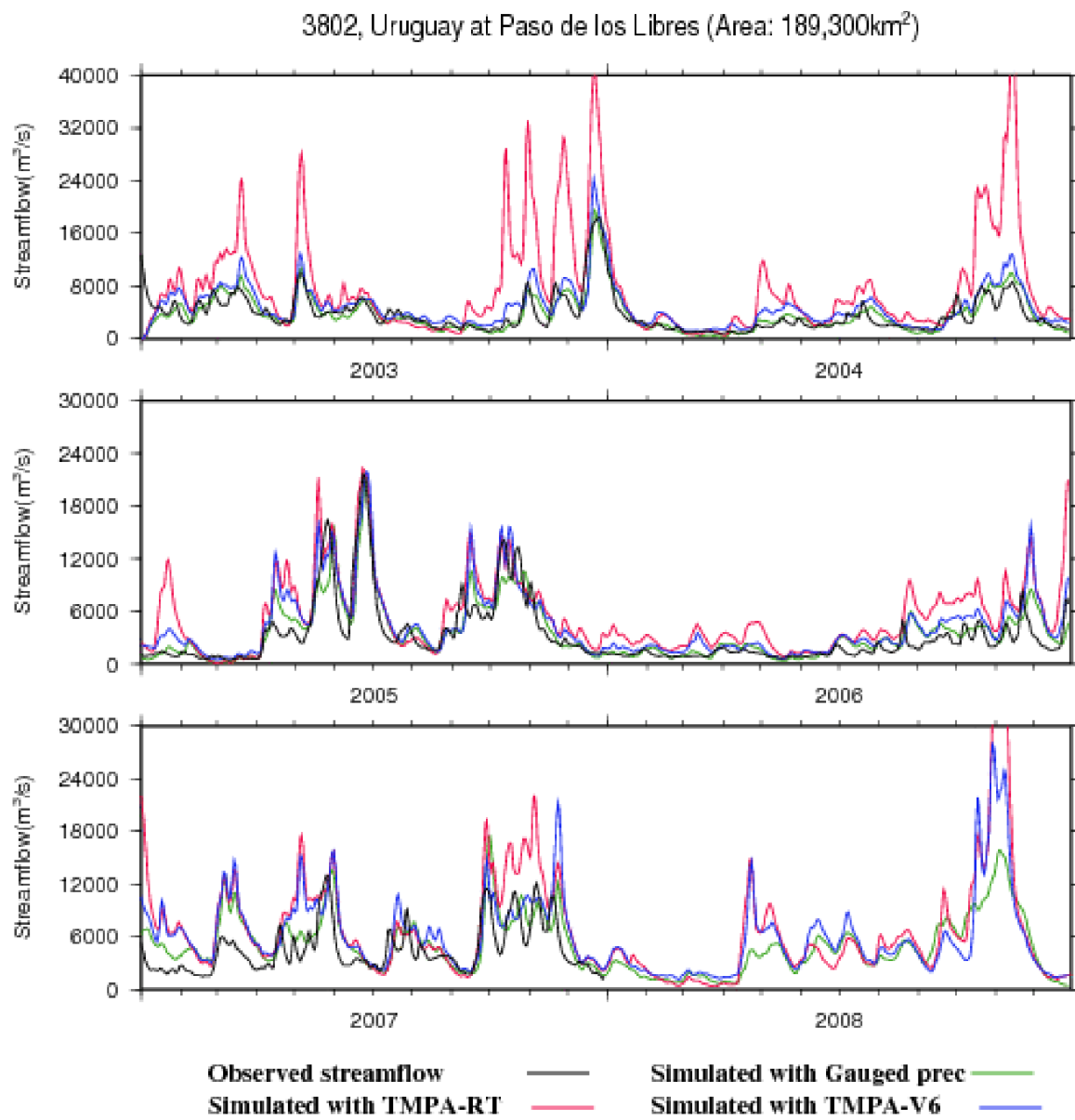


FIG. 6. Daily VIC simulated streamflow forced by TMPA-RT, TMPA-V6, and gridded gauge precipitation estimates for 2003-2008 for station 3802 (Uruguay at Paso de los Libres).

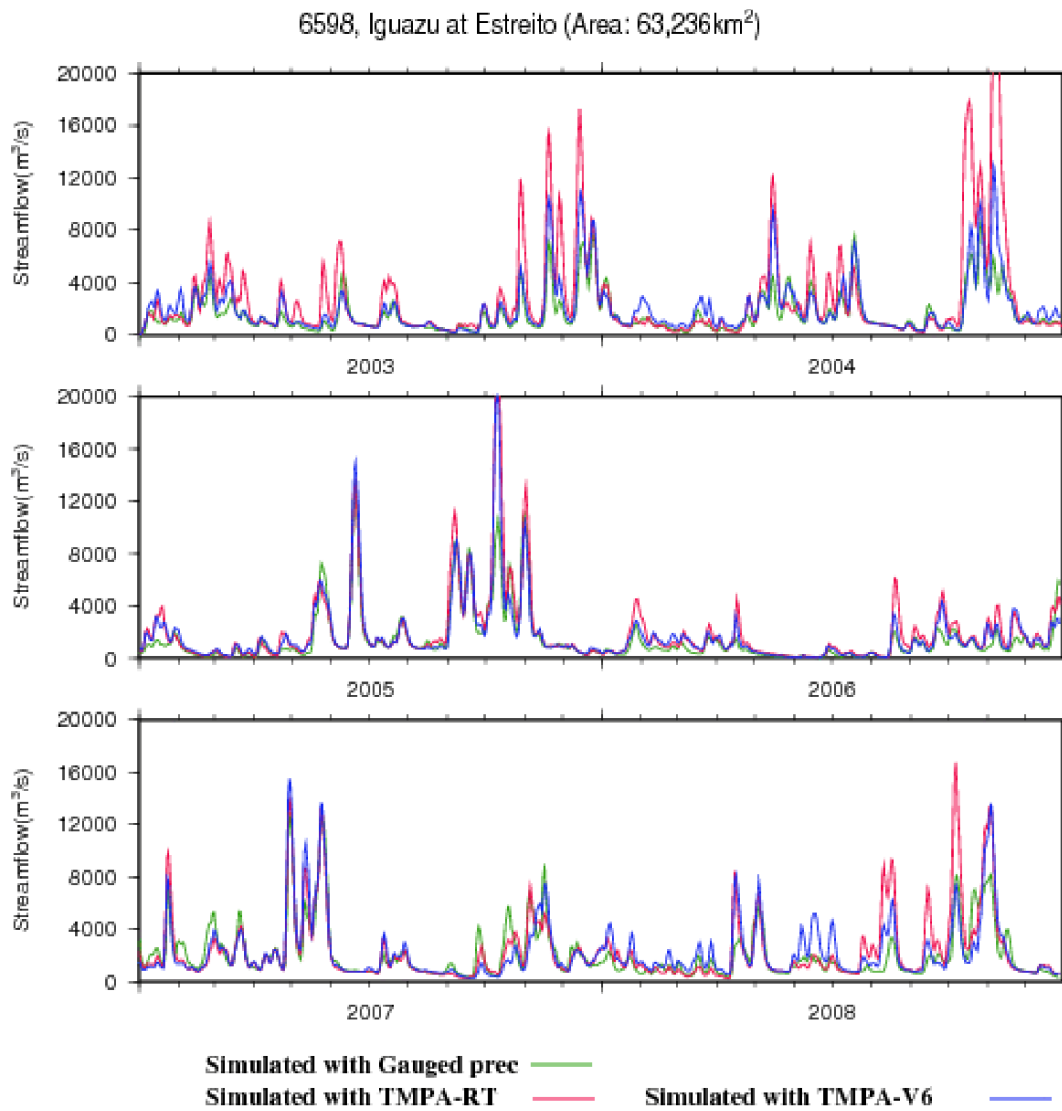


FIG.7. Same as Fig.6 but for basin 6598 (Iguazu at Estreito).

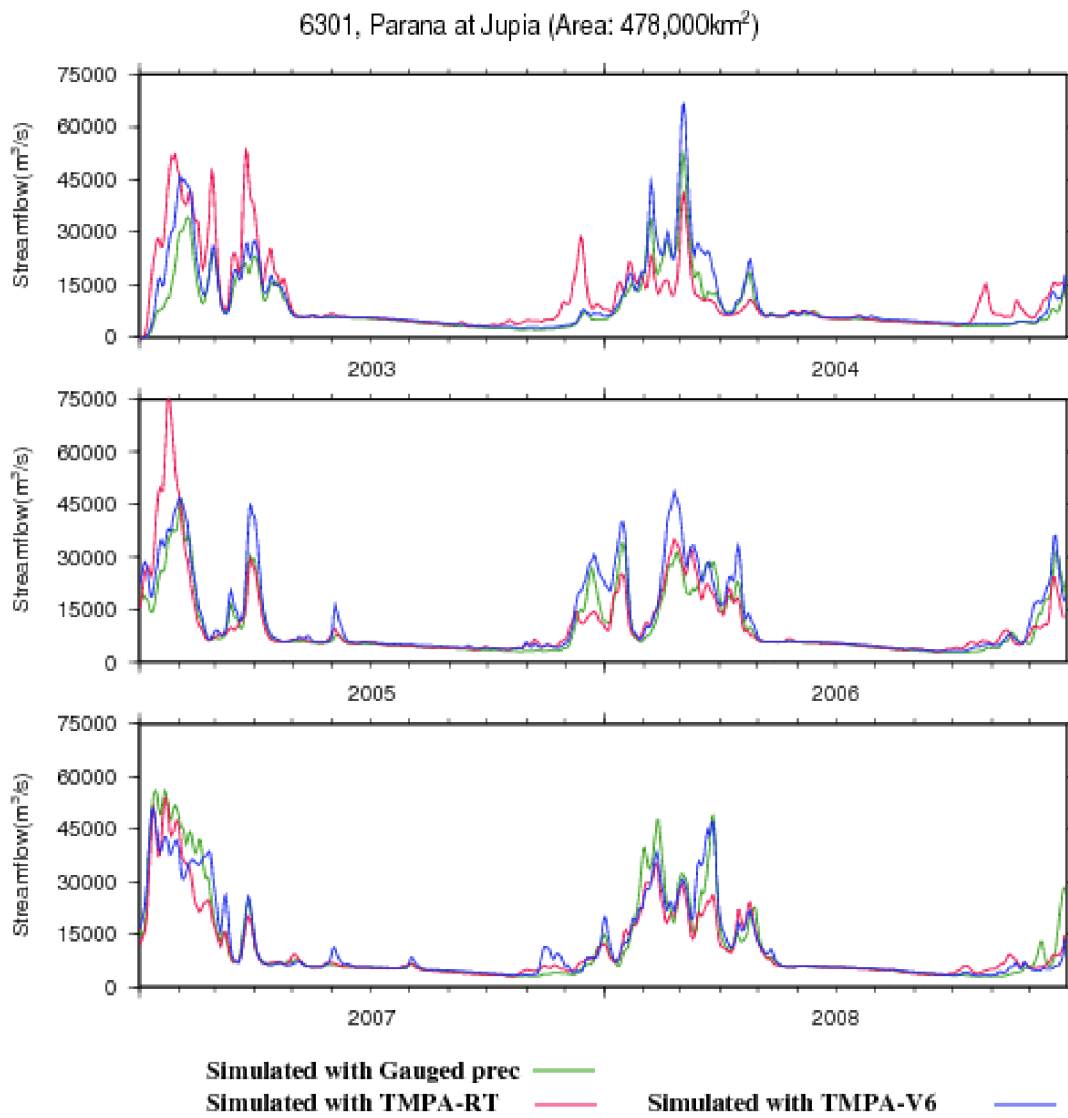


FIG 8. Same as Fig.6 but for basin 6301 (Parana at Jupia).

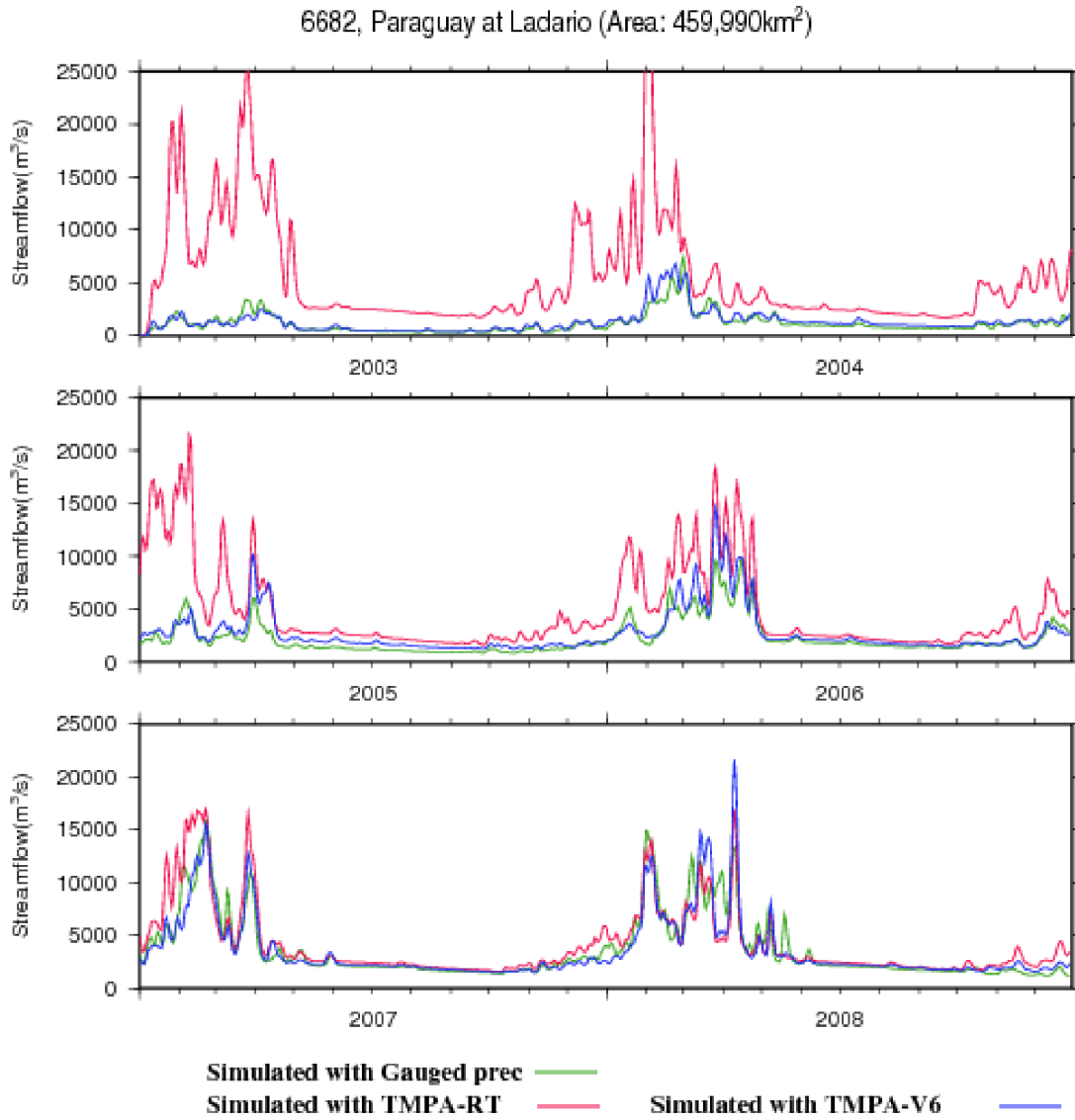


FIG. 9. Same as Fig.6 but for basin 6682 (Paraguay at Ladario).